Observations of the Askaryan Effect in Ice

P. W. Gorham,[1] S. W. Barwick,[2] J. J. Beatty,[3] D. Z. Besson,[4] W. R. Binns,[5] C. Chen,[6] P. Chen,[6] J. M. Clem,[7] A. Connolly,[8] P. F. Dowkontt,[5] M. A. DuVernois,[9] R. C. Field,[6] D. Goldstein,[2] A. Goodhue,[8] C. Hast,[6] C. L. Hebert,[1] S. Hoover,[8] M. H. Israel,[5] J. Kowalski,[1] J. G. Learned,[1] K. M. Liewer,[10] J. T. Link,[1,11] E. Lusczek,[9] S. Matsuno,[1] B. Mercurio,[3] C. Miki,[1] P. Miočinović,[1] J. Nam,[2] C. J. Naudet,[10] J. Ng,[6] R. Nichol,[3] K. Palladino,[3] K. Reil,[6] A. Romero-Wolf,[1] M. Rosen,[1] L. Ruckman,[1] D. Saltzberg,[8] D. Seckel,[7] G. S. Varner,[1] D. Walz,[6] and F. Wu[2]

(ANITA Collaboration)

[1]*Department of Physics and Astronomy, University of Hawaii, Manoa, Hawaii 96822, USA*
[2]*University of California, Irvine California 92697, USA*
[3]*Department of Physics, Ohio State University, Columbus, Ohio 43210, USA*
[4]*Department of Physics and Astronomy, University of Kansas, Lawrence, Kansas 66045, USA*
[5]*Department of Physics, Washington University in St. Louis, Missouri 63130, USA*
[6]*Stanford Linear Accelerator Center, Menlo Park, California, 94025, USA*
[7]*University of Delaware, Newark, Delaware 19716, USA*
[8]*Department of Physics and Astronomy, University of California, Los Angeles, California 90095, USA*
[9]*School of Physics and Astronomy, University of Minnesota, Minneapolis, Minnesota 55455, USA*
[10]*Jet Propulsion Laboratory, Pasadena, California 91109, USA*
[11]*Currently at NASA Goddard Space Flight Center, Greenbelt, Maryland, 20771, USA*

(Received 13 December 2006; revised manuscript received 15 June 2007; published 25 October 2007)

We report on observations of coherent, impulsive radio Cherenkov radiation from electromagnetic showers in solid ice. This is the first observation of the Askaryan effect in ice. As part of the complete validation process for the ANITA experiment, we performed an experiment at the Stanford Linear Accelerator Center in June 2006 using a 7.5 metric ton ice target. We measure for the first time the large-scale angular dependence of the radiation pattern, a major factor in determining the solid-angle acceptance of ultrahigh-energy neutrino detectors.

DOI: 10.1103/PhysRevLett.99.171101 PACS numbers: 95.55.Vj, 29.40.Ka, 98.70.Sa

Very large-scale detectors, such as the Antarctic Muon and Neutrino Detector Array and its successor IceCube, have demonstrated the excellent utility of Cherenkov radiation in detection of neutrino interactions at >TeV energies [1,2] with ice as a target medium. However, at neutrino energies above 100 PeV, the cubic-kilometer scale of such detectors is inadequate to detect more than a handful of events from the predicted cosmogenic neutrino fluxes [3] which represent the most compelling models at these energies. The relevant detector volume for convincing detection and characterization of these neutrinos is in the range of hundreds to thousands of km^3 of ice, and the economic constraints of scaling up the optical Cherenkov technique almost certainly preclude extending it much beyond the size of the current IceCube detector, which will be completed early in the next decade.

Given the need for an alternative technique with a more tractable economy of scale to reach into the EeV (=1000 PeV) energy regime, a new method has emerged within the last decade. This method, the radio Cherenkov technique, relies on properties of electromagnetic cascades in a dielectric medium. It was first hypothesized by Askaryan [4] and confirmed in 2001 at SLAC [5]. High energy processes such as Compton, Bhabha, and Møller scattering, and positron annihilation rapidly lead to a ~20% negative charge asymmetry in the electron-photon part of a cascade. In dense media the shower charge bunch is largely contained within a several cm radius. At wavelengths of ≥ 10 cm, much larger than the characteristic shower bunch size, the relativistic shower bunch appears as a single charge moving through the dielectric over a distance of several meters or more. As an example, a typical shower with mean Bjorken inelasticity $\langle y \rangle = 0.2$, initiated by a $E_\nu =$ 100 PeV neutrino creates a total number of charged particles at shower maximum of order $n_{e+} + n_{e-} = \langle y \rangle E_\nu / 1\ \mathrm{GeV} \sim 2 \times 10^7$. The net charge is thus $n_{e+} - n_{e-} \sim 4 \times 10^6 e$. Since the radiated power for Cherenkov emission grows quadratically with the charge of the emitter, the coherent power in the cm-to-m wavelength regime is $\sim 10^{13}$ times greater than the single-charge emission, far exceeding any other secondary emission in optical or longer-wave bands, and dominating other coherent radio emission processes in solids, such as transition radiation [6] and synchrotron radiation in the Earth's magnetic field [7].

To quantify these considerations we use a simple but reasonably accurate model for coherent radio Cherenkov emission produced by the Askaryan effect [8] based on a Gaussian profile for the longitudinal charge distribution along a shower. The radio frequency regime where full coherence obtains is given approximately by the requirement that $kL \gg 1$, where the wave number $k = n\omega/c$ and $n = \sqrt{\epsilon\mu}$ for frequency ω and index of refraction n, and L is a Gaussian parameter giving the characteristic longitudinal extent of the shower. In this regime, the Cherenkov field strength ($\mathrm{V\,m^{-1}\,Hz^{-1}}$) can be determined by transforming the current to determine the vector potential, which in turn gives a relation for the radiated emission. For consistency with existing literature [9], we define the electric field pulse spectrum as $\mathbf{E}(\omega) = 2\int_{-\infty}^{+\infty}\mathbf{E}(t)e^{i\omega t}dt$. For a model of the shower as a point charge moving at the speed of light with variable charge $q = q(z)$, the current is $J_z(\mathbf{r}, t) = cq(z)\delta(\mathbf{r} - c\hat{z}t)$ and $J_x = J_y = 0$. The Fourier transform (consistent with $\mathbf{E}(\omega)$ above) is $J_z(\mathbf{r}, \omega) = 2\int J_z e^{i\omega t}dt = 2q(z)\delta(x)\delta(y)e^{i\omega z/c}$. The frequency-domain vector potential $\mathbf{A}$ satisfies the Helmholtz equation $\nabla^2 A_z + k^2 A = -\mu\mu_0 J_z$ and $A_x = A_y = 0$. Its solution at the observation point $\mathbf{R}$ is $A_z(\mathbf{R}) = \mu\mu_0\int \exp(ikR')/(4\pi R')J_z(\mathbf{r})d^3\mathbf{r}$, where $R' = |\mathbf{R} - \mathbf{r}|$. In the Fraunhofer zone, the standard approximation is $\exp(ikR')/(4\pi R') \approx \exp(ikR)/(4\pi R)\exp[-i(\mathbf{k}\cdot\mathbf{r})]$. Thus,

$$A_z(\mathbf{R}, \omega) = \mu\mu_0 \frac{e^{ikR}}{2\pi R}\int_{-\infty}^{+\infty} q(z)e^{-iz(k\cos\theta-\omega/c)}dz$$

where θ is the polar emission angle. The magnetic induction is $\mathbf{B} = \nabla \times \mathbf{A}$. In the far zone $B = |\mathbf{B}| = kA_z\sin\theta$ and the electric field is $E = cB/n = \omega A_z\sin\theta$. For a Gaussian shower profile $q(z) = Q\exp[-(z - z_{\max})^2/2L^2]$, where Q is the maximum attained charge excess and L is the characteristic shower length. Then

$$|R\mathbf{E}(f)| = \sqrt{2\pi}\mu\mu_0 QLf\sin\theta e^{-(kL)^2(\cos\theta-1/n)^2/2}, \tag{1}$$

where for typical dielectrics $\mu = 1$, $\mu_0 = 4\pi\times 10^{-7}$ is the permeability of free space. Equation (1) provides an analytic form for evaluating emission from this process, once L and Q are determined via Monte Carlo simulations or existing shower parametrizations.

In the mid-to-late 1980s, proposals to observe Askaryan impulses from neutrino interactions in Antarctic ice [10–12] and the Lunar regolith [13] created a renewed interest in Askaryan's work. In the early 1990s, the first comprehensive effort to combine EM shower simulations in ice with electrodynamics resulted in strong support for the validity of the methods [9], and in the later 1990s the Radio Ice Cherenkov Experiment (RICE) [14], and Goldstone Lunar Ultrahigh-energy neutrino Experiment (GLUE) [15] began operation of experiments designed to exploit the effect. The first laboratory tests of the Askaryan effect took place in 1999–2000 [5,6] using silica sand, followed by subsequent measurements in rock salt in 2002 [16,17]. Since then, the Fast On-orbit Recorder of Transient Events (FORTE) [8] satellite and the Antarctic Impulsive Transient Antenna (ANITA) [18] experiment have now extended the method to synoptic spacecraft and balloon-payload observations of ultralarge volumes of the Greenland or Antarctic ice sheets.

There are important reasons to test Askaryan's theory in ice as well as sand and salt, since so much study and experimental effort have considered ice as the target medium. First, although the effect is primarily determined by shower physics, the radio production and transmission occurs under conditions where the properties of the medium could modify the behavior of the emission; the possibility of unknown media-dependent effects which might suppress the emission must be explored. Second, the radio Cherenkov method is most effective at shower energies above 10–100 PeV, where muon or other cosmic-ray backgrounds are negligible. The method thus has the virtue of having no known physics backgrounds, but neither can it use such backgrounds to calibrate the Cherenkov intensity and corresponding detection efficiency. In this context, laboratory calibrations of the radiation behavior are critical to the reliability of results. And finally, the increased richness of these radio observations, which directly measure electric field strength and vector polarization, require more comprehensive experimental treatment and validation than observations of scalar intensity.

The experiment, SLAC T486, was performed in the End Station A (ESA) facility during the period from June 19–24, 2006. A target of very pure carving-grade ice was constructed from close packing rectangular 136 kg blocks (about 55 were used) to form a stack approximately 2 m wide by 1.5 m tall (at the beam entrance) by 5 m long. The upper surface of the ice was carved to a slope of ~8° in the forward direction giving the block a trapezoidal longitudinal cross section along the beam axis. This was done to avoid total-internal reflection (TIR), of the emerging Cherenkov radiation at the surface. The surface after carving was measured to have a root-mean-square roughness of 2.3 cm. The beam entered this target about 40 cm above the target floor, which was lined with ferrite tiles to suppress reflections off the bottom. The showers were produced by 28.5 GeV electrons in 10 picosecond bunches of typically 10^9 particles. Monte Carlo simulations of the showers indicate that about 90% of the shower was contained in the target; the remainder was dumped into a pair of downstream concrete blocks. The transverse radius of the shower is several cm at most; this parameter also justifies the high degree of coherence observed in our frequency regime, and the use of Eq. (1) above. In contrast to previous experiments [5,16], we did not convert the electrons to

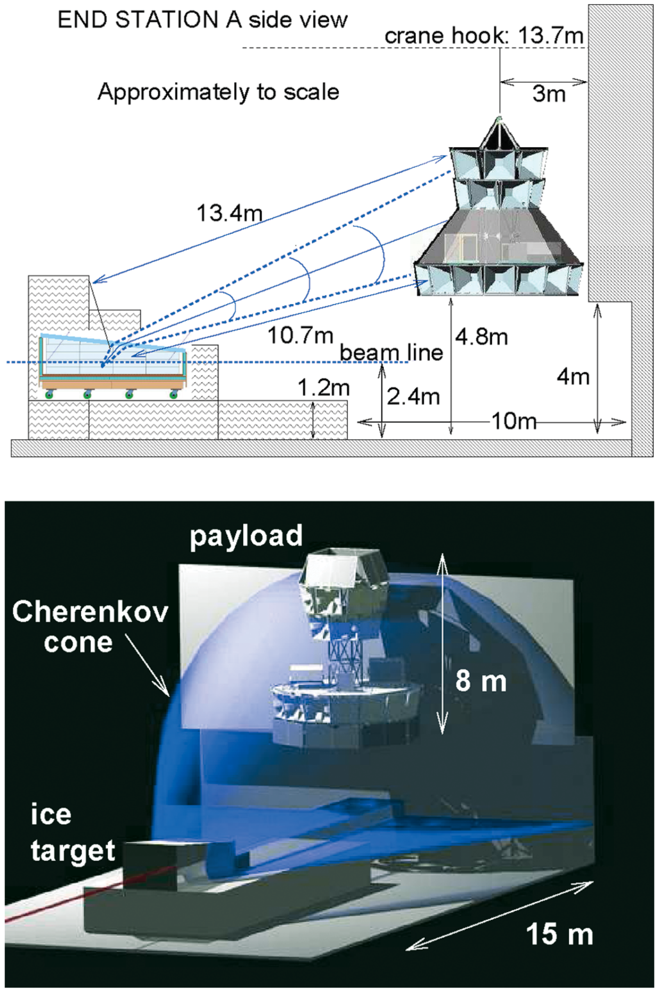

FIG. 1 (color). Top: Side view schematic of the target and receiver arrangement in ESA. Bottom: Perspective view of the setup, showing the key elements.

photons via a bremsstrahlung radiator. Such methods were used in earlier Askaryan discovery experiments to avoid any initial excess charge in the shower development. In our case, the typical shower had a total composite energy of 3×10^{19} eV, with a total of $\sim 2 \times 10^{10} e^+e^-$ pairs at shower maximum. Simulations of the charge excess development indicate a net charge asymmetry of about 20%. Thus the initial electrons contribute at most ~15% of the total negative charge excess in the shower, and we have corrected for this bias in the results we show here. In addition, radio-absorbing foam was in place on the front face of the ice, and very effectively suppressed rf noise from the upstream metal beam vacuum windows and air gaps. Our previous experiments [5,16] measured accelerator rf backgrounds at SLAC, and they are a negligible contribution to our measurements. A schematic and perspective view of the experiment layout is shown in Fig. 1. The ice was contained in a 10 cm thick insulating foam-lined box, and a 10 cm foam lid was used during operation, along with a freezer unit, to maintain temperatures of between -5 to $-20\,^{\circ}\mathrm{C}$. Such temperatures are adequate to avoid significant rf absorption over the several m pathlengths of the radiation through the ice [19].

The ANITA payload (Fig. 2, consisting of an array of 32 dual-polarization quad-ridged horns along with eight omnidirectional conical antennas, was used to receive the emission at a location about 15 m away from the center of the target, as shown in Fig. 1. The antenna frequency range is from 200–1200 MHz, a frequency range over which the rf transmissivity of ice is at its highest [19]. ANITA horn antennas are arranged so that adjacent antennas in both the lower and upper payload sections respond well even to a signal directed along their nearest neighbors' bore sights. This allows multiple antennas (typically 4 to 6 horns and 3 to 4 of the conical antennas) to sample the arriving wave front. The signals are digitized by custom compact-PCI-based 8-channel digitizer modules [20], 9 of which are used to record all 72 antenna signals simultaneously at 2.6 G samples/ sec .

Figure 3 (left) presents results for the absolute field strength of the radio impulse in the several different antennas employed here, with uncertainties of about ±40% in field strength (±3 dB), dominated by systematic rather than statistical errors, arising from a combination of the 1–2 dB uncertainty in the gain calibration of the antennas, and by comparable uncertainties in removing secondary reflections from the measured impulse power. The field strengths are compared to a parametrization based on shower + electrodynamics simulations for ice [9], and the agreement is well within our experimental errors. Figure 3 (right) shows results of the scaling of the pulse power with shower energy. The dependence is completely consistent with quadratic scaling, indicating that the radiation is coherent over the 200–1200 MHz frequency window.

Figure 4 shows the measured and predicted angular dependence of the radiation, for data up to 800 MHz; beyond this the SNR of the data was inadequate for such sub-band analysis. The Cherenkov cone refracts into the forward direction out of the ice, and is clearly delineated by the data. Here we show statistical + systematic errors within a measurement run; the overall normalization (with separate systematic error) is taken from Fig. 3. We scale these data within the overall systematic errors to match the peak of the field strength. For T486, $L \sim 1.2$ m for Eq. (1) above. The measured angular dependence follows closely the expectations for Cherenkov radiation, including the narrowing of the Cherenkov cone with higher frequencies. This behavior arises from the kL term in the exponential of Eq. (1), and is important since the width of the Cherenkov cone determines the detection solid angle, or *acceptance* of a high energy neutrino detector. This measurement confirms the predicted behavior for the first time.

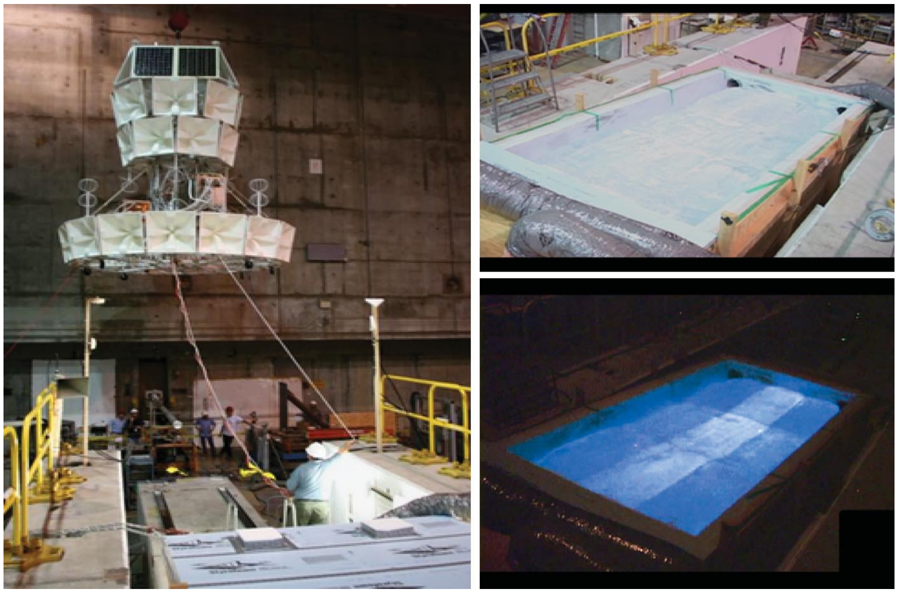

FIG. 2 (color). Left: The ANITA payload (center) above and downstream of the ice target (here covered). Right top, target with cover removed, in ambient light. Right bottom: ice target illuminated from interior scattered optical Cherenkov radiation.

In summary, Askaryan's hypothesis has now been confirmed in detail by laboratory experiments for virtually all of the dielectrics (ice, salt, sand—the latter approximating the Lunar regolith) that Askaryan envisioned as the best media in which to exploit the coherent radio Cherenkov emission from high energy particle showers. Askaryan's intent was to illuminate a methodology by which low fluxes of ultrahigh-energy particles could be made observable through exploitation of huge volumes of natural materials. With the recent sharpening of predictions for the fluxes of ultrahigh-energy neutrinos, and the growth in the number of experiments that make use of it, we expect that Askaryan's hope will be soon fulfilled.

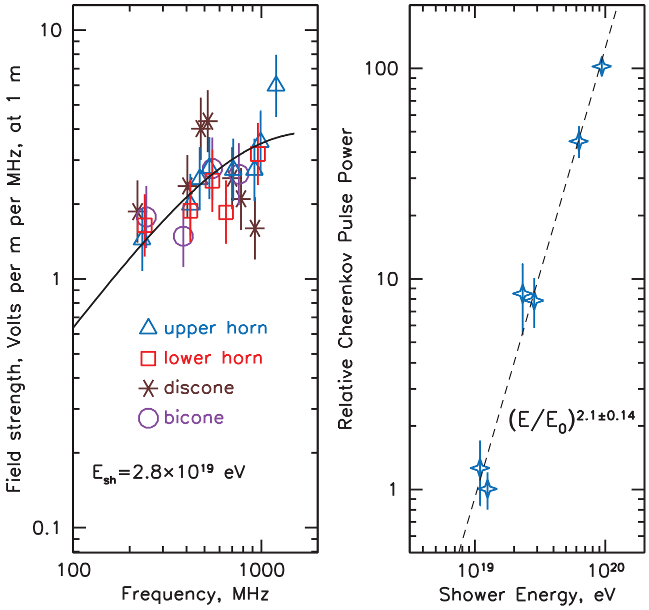

FIG. 3 (color). Left: Field strength vs frequency of radio Cherenkov radiation in the T486 experiment, for several different antennas used, including a theoretical curve [9]. Right: Pulse power vs total shower energy (number of particles × mean energy/particle), curve is for completely coherent radio Cherenkov emission.

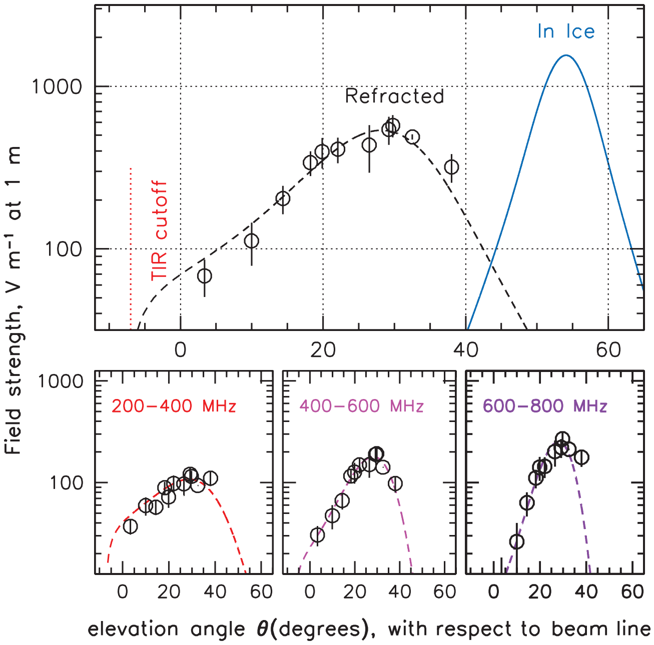

FIG. 4 (color). Top: Angular dependence of the radiation for both the in-ice and refracted case, for a frequency range from 200–800 MHz, compared to data. The data errors are combined statistical and systematic, but with an arbitrary overall normalization-see Fig. 3 for the normalization factor. The in-ice and refracted curves are the theoretical expectation for a shower in ice at a beam current of $10^9 e^-$ per bunch and 28.5 GeV electrons, and the refraction includes only geometric optics. Bottom: Same as top for three different subfrequency bands.

This work has been supported by the National Aeronautics and Space Administration and the Department of Energy , Office of Science, High Energy Physics Division. We thank the SLAC Experimental Facilities Department and the Columbia Scientific Balloon Facility for their invaluable support. Special thanks to Thermo King Services of San Leandro, CA and Glacier Ice of Fremont, CA.

---

[1] J. Ahrens *et al.* (AMANDA Collaboration), Nucl. Instrum. Methods Phys. Res., Sect. A **524**, 169 (2004).
[2] M. Ackermann *et al.* (IceCube Collaboration), Nucl. Instrum. Methods Phys. Res., Sect. A **556**, 169 (2006).
[3] V. S. Beresinsky and G. T. Zatsepin, Phys. Lett. B **28**, 423 (1969); R. Engel, D. Seckel, and T. Stanev, Phys. Rev. D **64**, 093010 (2001).
[4] G. A. Askaryan, JETP **14**, 441 (1962); **21**, 658 (1965).
[5] D. Saltzberg, P. Gorham, and D. Walz *et al.*, Phys. Rev. Lett. **86**, 2802 (2001).
[6] P. W. Gorham, D. P. Saltzberg, and P. Schoessow *et al.*, Phys. Rev. E **62**, 8590 (2000).
[7] Y. Shibata *et al.*, Phys. Rev. A **44**, R3449 (1991).
[8] N. Lehtinen, P. Gorham, A. Jacobson, and R. Roussel-Dupré, Phys. Rev. D **69**, 013008 (2004); arXiv:astro-ph/030965.
[9] E. Zas, F. Halzen, and T. Stanev, Phys. Rev. D **45**, 362 (1992); J. Alvarez-Muñiz and E. Zas, Phys. Lett. B **411**, 218 (1997).
[10] G. A. Gusev and I. M. Zheleznykh, Sov. Phys. Usp. **27**, 550 (1984).
[11] M. A. Markov and I. M. Zheleznykh, Nucl. Instrum. Methods Phys. Res., Sect. A **248**, 242 (1986).
[12] M. A. Markov, *Proceedings of the 10th International Conference on High Energy Physics, Rochester, 1960* (University of Rochester, Rochester, 1960) p. 578; M. A. Markov, I. M. Zheleznykh, Nucl. Phys. **27**, 385 (1961).
[13] I. M. Zheleznykh, Proc. Neutrino **88**, 528 (1988); R. D. Dagkesamanskii and I. M. Zheleznyk, JETP **50**, 233 (1989).
[14] I. Kravchenko *et al.*, Astropart. Phys. **20**, 195 (2003).
[15] P. W. Gorham, C. L. Hebert, K. M. Liewer, C. J. Naudet, D. Saltzberg, and D. Williams, Phys. Rev. Lett. **93**, 041101 (2004).
[16] P. W. Gorham, D. Saltzberg, and R. C. Field *et al.*, Phys. Rev. D **72**, 023002 (2005).
[17] P. Miočinović, R. C. Field, and P. W. Gorham *et al.*, Phys. Rev. D **74**, 043002 (2006).
[18] S. W. Barwick *et al.* (The ANITA Collaboration), Phys. Rev. Lett. **96**, 171101 (2006).
[19] S. Barwick, D. Besson, P. Gorham, and D. Saltzberg, J. Glaciol. **51**, 231 (2005).
[20] G. Varner *et al.*, "The Large Analog Bandwidth Recorder and Digitizer with Ordered Readout (LABRADOR) ASIC," Nucl. Instrum. Methods Phys. Res., Sect. A (to be published).